Concentration Dependence of the Relative Viscosity of Star Polymers†

Jacques Roovers

Institute for Environmental Chemistry, National Research Council of Canada, Ottawa, Ontario, Canada K1A 0R6

Received April 4, 1994; Revised Manuscript Received June 15, 1994®

ABSTRACT: The concentration dependence of the relative viscosities of polybutadiene star polymers with 64, 128 and 270 arms has been investigated in the good solvent toluene. It is shown that the viscosity-concentration behavior of these stars matches that of hard-sphere suspensions. Near the overlap concentration c*, the star polymers form physical gels similar to the behavior of hard-spheres at the close packing volume fraction. Blending of two 128-arm stars with a large differences in size reduces the viscosity of the solutions and delays the gel formation to higher concentration. A sufficiently high segment density in the outer corona of the polymer coils is required in order to observe the hard-sphere viscosity-concentration profiles as demonstrated by the results on 32-arm stars and fuzzy 64-arm stars with 32-arms in the corona. In the case of a poly(butadiene-b-styrene) star a weak increase of the relative viscosity is observed at concentrations between two and three times the overlap concentration.

Introduction

The synthesis and dilute solution characterization of regular star polymers with 64 and 128 arms have been described.[1] Because a large number of arms are joined to a small dendritic core, the segment density in the polymer coils is very high. The properties of these star polymers suggest that they behave much like hard-sphere particles in dilute solution. For example, the hydrodynamic and thermodynamic radii obey

$$R_V = R_T \approx (5/3)^{1/2} R_G \qquad (1)$$

where R_G is the radius of gyration. The numerical coefficient in eq 1 is typical of equal-density hard-sphere particles. Furthermore, the Huggins constant of the star polymers approaches unity with increasing number of arms, f, in the star.[2] In a recent SANS study of the single particle scattering function (the form factor), the sphere-like conformation is shown to increase strongly with f, and it is sufficiently well developed for $f = 128$ that a weak secondary maximum is observed in the scattering.[3] The scattering function is also consistent with a rather sharp dropoff of the segment density at the periphery of stars with many arms. Of course, the equal-density hard-sphere model is an approximation because the star polymer coils are swollen with solvent, and the segment density distribution within the coil decreases from the core to the periphery according to the Daoud–Cotton model.[1,4] Nevertheless, in good solvents there is a strong repulsion between the polymer coils due to the high internal osmotic pressure that extends to the coil periphery.[5] The intermolecular interactions, characterized by strong repulsion, cause ordering of the polymer coils. This is experimentally manifested by a strong Bragg peak in SANS of stars with many arms near the overlap concentration and in semidilute solution.[6] The characteristic distance associated with the Bragg peak is on the order of the star polymer diameter. The ordering in solutions of star polymers is macroscopically revealed by their gellike properties. Gel formation near the overlap concentration is similar to the behavior of a suspension of hard spheres near the close-packing volume fraction.

In this study the concentration dependence of the Newtonian viscosity of star polymers in a good solvent is investigated up to the gel point. The concentration dependence of the viscosity is compared to that of real hard-sphere particles.[7–9] The dependence on molecular weight, number of arms, polydispersity, and surface fuzziness of the stars is described. Some measurements have also been made on a poly(butadiene-*b*-styrene) star.

Experimental Section

The synthesis of regular polybutadiene star polymers with 64 and 128 arms has been described.[1] The arms of the stars are prepared anionically with *sec*-BuLi in benzene and coupled with a dendrimer containing 64 or 128 peripheral Si–Cl bonds.[10] Star polymers with 32 arms were prepared in a similar way.[11] Two samples of star polymers with 270 arms[12] are also used in this study. They are not regular star polymers because they are synthesized by coupling living polybutadiene onto a small linear backbone containing 135 $CH_2CH_2Si(CH_3)Cl_2$ groups.[12] Two 64-arm star polybutadienes with a fuzzy surface were prepared by first coupling 32 arms of a 60 000 polybutadiene followed by 32 arms with 42 000 or 22 000. The two samples are identified by 646042 and 646022, respectively.[13] The preparation of the star block copolymer 641020 was by the coupling of living poly(styrene-*b*-butadienyllithium) with the dendrimer containing 64 Si–Cl bonds. The outer corona of the star polymer consists of 64 blocks of polystyrene each with MW = 10 000, and the inner core is formed by polybutadiene blocks with MW = 20 000.

Solutions of the star polymers in toluene were prepared by weight. Additivity of volumes was assumed. The density of polybutadiene is 0.890 g/mL. The density of toluene at 35 °C is 0.853 g/mL. Sufficient time was allowed and slow rotation of the mixtures was used to speed the dissolution process.

Zero-shear viscosities were measured in calibrated semi-micro dilution Cannon–Ubbelohde viscometers at 35 °C. The viscosity of toluene is 0.493 cP. The maximum shear rate at the wall was calculated from[14]

$$\dot{\gamma} = 4Q/\pi R^3 \ (\mathrm{s}^{-1}) \qquad (2)$$

where Q is the volume rate of flow and R is the radius of the capillary. In many cases $\dot{\gamma}$ was low because very long elution times (1–2 h) were recorded. The shear rate independence was checked by using different viscometers with different capillary radii. This was especially important for solutions near the gel point. Dilutions were made in the viscometer by the addition of weighed amounts of solvent. Gels were recognized by their yield stress and their curdlike appearance when shaken. The gels are extremely shear sensitive and are not further considered.

---

† Issued as NRCC No. 37567.

® Abstract published in *Advance ACS Abstracts*, August 1, 1994.

0024-9297/94/2227-5359$04.50/0

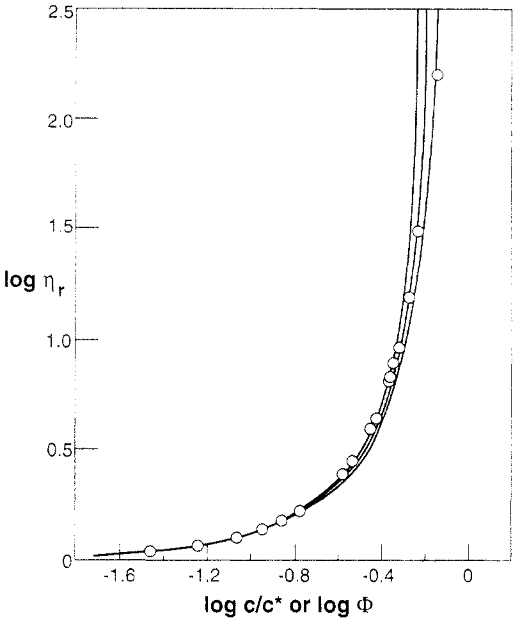

Figure 1. Double-logarithmic plot of the relative viscosity against the volume fraction of 128-arm star 12880. The lines represent eq 4 with, from left to right, ϕ_p = 0.59, 0.65, and 0.74.

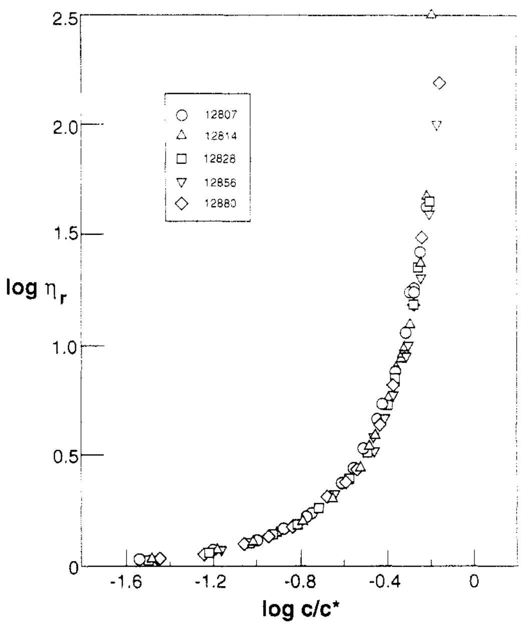

Figure 2. Effect of molecular weight on the relative viscosity of 128-arm star polymers. The concentration of each star polymer is scaled by its overlap concentration (eq 3).

Results

1. Regular Star Polymers. A typical concentration dependence of the relative Newtonian viscosity $\eta_r = \eta/\eta_s$, where η_s is the solvent viscosity, is shown in Figure 1 for the case of a 128-arm star polybutadiene. In Figure 1, η_r is plotted double-logarithmically against the polymer volume fraction c/c^*, where c^* is the overlap concentration defined by

$$c^* = [(N_A/M)(4\pi/3)R_V^{\,3}]^{-1} \qquad (3)$$

with N_A Avogadro's number, M the molecular weight, and R_V the viscosimetric equivalent hard-sphere radius of the polymer coil. It is easily shown that $1/c^* \approx 0.4[\eta]$. In this definition of the polymer volume fraction, the solvent within the polymer coil is an integral part of the polymer particle. We must keep in mind that the polymer coils shrink and interpenetrate each other under certain conditions. Therefore, c^* does not represent a physical limit to the polymer concentration.

The experimental data are compared with an equation proposed by Krieger and Dougherty for colloidal particles[7]

$$\eta_r = [1 - \phi/\phi_p]^{-[\eta]\phi_p} \qquad (4)$$

where ϕ is the volume fraction, ϕ_p is the close-packing volume fraction of the hard spheres, and $[\eta]$ = 2.5 is the Einstein value for their intrinsic viscosity. Equation 4 has only one adjustable parameter ϕ_p and is based on a mean-field approach in which an existing suspension of particles acts as a continuous medium for the added particles. It includes a factor ϕ_p to take into account the crowding that gradually increases with the concentration of the particles.[8] From Figure 1 it can be seen that eq 4 with $0.59 < \phi_p < 0.65$ describes reasonably well the experimental results over most of the concentration range. A value of $\phi_p \approx 0.60$ is typical of random close packing. Random close packing of the star polymer coils agrees qualitatively with the absence of clear multiple Bragg scattering maxima in SANS experiments on these polymers in semidilute solution.[6]

It can be seen in Figure 1 that the highest concentration point at c/c^* = 0.71 deviates from eq 4. This could be due to a failure of eq 4 to describe the viscosity–concentration dependence correctly close to ϕ_p. Alternatively, it suggests that a small reduction of R_V (and increase in c^*) may be necessary to take into account a slight softness of the star polymer periphery.[15] However, applying a smaller effective radius to calculate c^* upsets the good fit over the whole lower concentration range. It seems therefore that the lower viscosity at concentrations near ϕ_p is specific to that concentration range. From SANS measurements it is expected that the radius of gyration of 128-arm stars does not shrink in the concentration range over which the viscosities are measured.[3] This suggests then that the star polymers slightly interpenetrate each other before the physical gel point is reached. It can be estimated that the interpenetration would amount to only 3% of the star polymer radius.

The effect of molecular weight on the viscosity–concentration dependence of 128-arm star polymers is shown in Figure 2. The overlap concentration c^* of each polymer has been calculated with eq 3. Values of $[\eta]$ and M_w are given in Table 1. Figure 2 shows that the viscosities of all samples scale identically with c^*. The deviations from eq 4 observed at high polymer volume fraction are also common to all samples. In order to investigate this point in more detail, the highest observed volume fraction at which the solution is liquid and the lowest volume fraction at which a gel has been observed are plotted in Figure 3 as a function of the molecular weight of the 128-arm star polymer. It appears that the volume fraction of the liquid–gel transition increases from $c/c^* \simeq 0.64$ to 0.72 over a 10-fold molecular weight increase. This is in agreement with the expectation that stars with larger arms are hydrodynamically softer than star polymers with short arms. Numerical details of this liquid–gel transition are given in Table 1.

The experimental viscosity–concentration data for polybutadiene star polymers with 64 arms are shown in Figure 4. For comparison, a curve representing eq 4 with ϕ_p = 0.65 is included. It is obvious that departures from the classical hard-sphere behavior occur at lower c/c^* and are more important than in the case of 128-arm stars. The

Table 1. Viscosity–Concentration Characteristics of Star Polymers

			liquid		gel	
sample	$M_w \times 10^{-5}$	$[\eta]_{\mathrm{Tol}}^{35\,°\mathrm{C}}$ (mL/g)	c/c^*	$\log \eta_r$	c (g/mL)	c/c^*
12807	8.4	25.8	0.610	1.623	0.0630	0.650
12814	16.2	42.8	0.660	2.518	0.0416	0.712
12828	29.8	69.3	0.621	1.667	0.0248	0.690
12856	59.5	114.9	0.690	1.999	0.0166	0.761
12880	88.0	152.2	0.709	2.191	0.0131	0.797
6407	3.9_5	28.7	0.809	1.575	0.11[a]	1.263[a]
6415	7.2_5	43.2	0.685	1.347		
6430	13.4	70.5	0.879	1.765	0.0343	0.966
6460	28.9	126	0.937	2.785	0.0195	0.983
6480	42.0	166	0.844	1.783		
3220[b]	6.4_4	72				
3280[b]	30.1	218				
LS3B3[c]	26.0	36.2	0.696	1.954		
LS6B3[c]	112.0	97.5	0.664	2.240	0.0179	0.697
646022[d]		161.0				
646042[d]		165.5				
12880/07(9)[e]	8.1	135.6	0.77	2.279	0.0162	0.880
12880/07(50)[e]	4.8	92.0	1.15	1.723	0.0356	1.310

[a] Observed during SANS measurements.[3,6] [b] No gel observed. [c] Reference 12. [d] Fuzzy 64-arm stars with 32 arms of 60 000 and 32 arms of 22 000 and 42 000, respectively. [e] Blends of 12880 with 9% 12807 and 50% 12807, respectively.

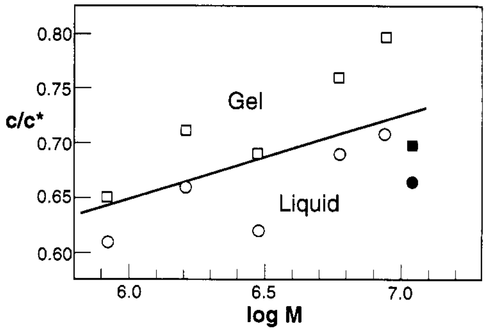

Figure 3. Effect of molecular weight on the liquid–gel transition of 128-arm star polymers. Circles: liquid samples. Squares: gel behavior observed in the sample. The full symbols are for LS6B3 which contains 270 arms.

liquid–gel transition of the 64-arm stars is observed in the range 0.90 < c/c^* < 1.0 which is higher than that for the 128-arm stars.

The viscosity–concentration data obtained for 32-arm star polybutadienes are shown in Figure 5 up to $c = 2.5c^*$. Equation 4 with $\phi_p = 0.65$ does no longer describe the experimental results above $c/c^* = 0.5$. The viscosity is much lower, and at no concentration is gelation of 32-arm star polymer solutions observed. It is therefore expected that the viscosity of 32-arm star polymers increases monotonically with concentration to the melt viscosity.[16] A line representing experimental data for linear polymers in a good solvent is included in Figure 5. The viscosity–concentration dependence of linear polymers and star polymers with 4 and 6 arms has been studied extensively previously.[17-19]

2. Multiarm Star Polymers. The synthesis and characterization of the star polymers with 270 arms have been described previously.[12] Depending on whether the linear polymer backbone, which forms the core of these polymers, is highly coiled or stretched, these polymers are expected to have a highly spherical conformation or the shape of hairy caterpillars. In the latter conformation they would form polymeric analogues of rodlike micelles. No clear experimental evidence is as yet available to differentiate between these two possible conformations. Values of R_G and R_V of these multiarm star polymers are somewhat larger than expected from an extrapolation of the data of other regular star polymers with 18–128 arms.[1] This suggests that the conformation of these multiarm stars is not exactly identical to that of regular star polymers. The concentration dependence of the relative viscosity of two samples is shown in Figure 6. Within experimental error both sets of data adhere well to the Krieger–Dougherty model with $\phi_p = 0.65$. Both samples form gels at high concentrations. The liquid–gel transition of LS6B3 at $c/c^* \approx 0.67$ is also shown in Figure 3. It is slightly lower than for the 128-arm star with similar molecular weight and, therefore, in qualitative agreement with the trend observed in the case of the 64- and 128-arm stars. It provides further evidence that the minimum value for the liquid–gel transition of star polymers is approximately at $c/c^* \approx 0.65$ which is consistent with the use of $\phi_p = 0.65$ in eq 4 to model the viscosity–concentration dependence.

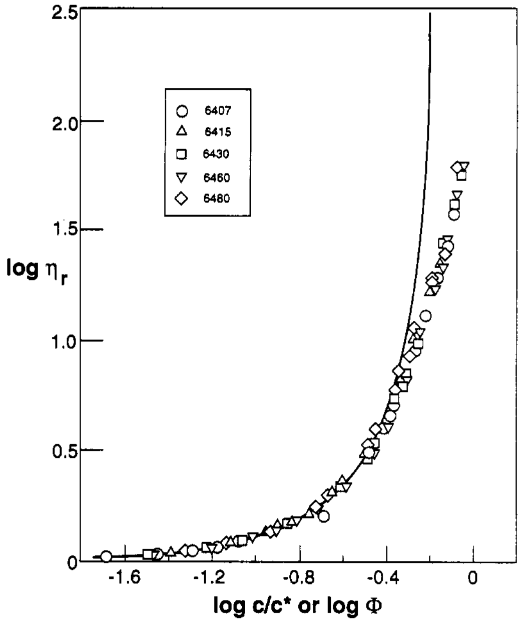

Figure 4. Double-logarithmic plot of the relative viscosity against volume fraction of 64-arm star polymers. The line represents eq 4 with $\phi_p = 0.65$.

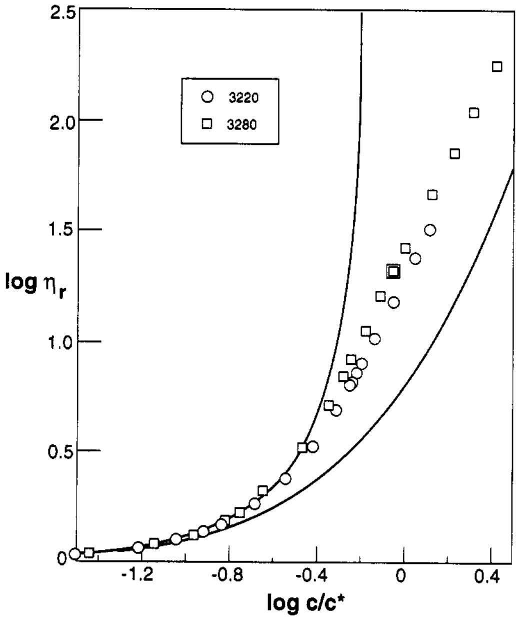

Figure 5. Double-logarithmic plot of the relative viscosity against the volume fraction for 32-arm star polymers. Maximum $c/c^* = 2.5$. The top line represents eq 4 with $\phi_p = 0.65$. The lower line represents data for linear polymers in a good solvent.

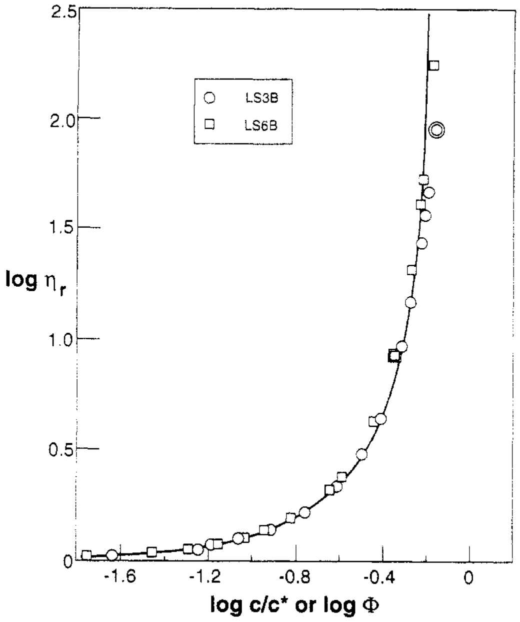

Figure 6. Plot of the relative viscosity against volume fraction for 270-arm star polybutadienes. The line represents eq 4 with $\phi_p = 0.65$.

3. Effect of Polydispersity. In order to study the effect of polydispersity on the concentration dependence of the viscosity, blends of two star polymers with 128 arms have been prepared. In one blend polybutadiene 12880 was mixed with 9% by weight of 12807. This constitutes a mixture with equal numbers of each polymer. The other blend is a 50/50 (w/w) mixture of the same two polymers. This blend contains therefore approximately 10 times more small stars than large stars. The calculated weight-average MW and the experimental intrinsic viscosities of the two blends are given in Table 1. By comparison of the results given in Figure 7 with those of Figures 1 and 2, it can be seen that, at high volume fractions, the relative viscosities of solutions of blends of 128-arm stars are appreciably lower than those for single star solutions.

Farris showed that the relative viscosity of bimodal blends of non-interacting solid spherical particles is given by[20]

$$\eta_{r,bl} = \eta_r(\phi_S)\,\eta_r(\phi_L) < \eta_r(\phi_T) \qquad (5)$$

where $\phi_S = V_S/(V_0 + V_S)$, $\phi_L = V_L/(V_0 + V_S + V_L)$, and $\phi_T = (V_S + V_L)/(V_0 + V_S + V_L)$ with V_0, V_S, and V_L the solvent, small particle, and large particle volumes, respectively, and $\eta_r(\phi)$ is calculated with eq 4. Equation 5 is especially useful when the small to large sphere size ratio is 0.1 or less. The blending rule of eq 5 assumes essentially that the solution of small particles forms a continuous medium for the large particles (the mean-field approximation). For the star polymers in the blend studied here the size (diameter) ratio is 0.25. Equation 5 is compared with the experimental data for the 50/50 blend of 12807 and 12880 in Figure 8. Equation 5 clearly overestimates the relative viscosity of the blend of the two stars. Furthermore, the gel point of the 50/50 blend is predicted at $\phi_T = 0.70$, whereas experimentally, gel formation is observed at $1.2 < c/c^* < 1.3$. In contrast to gels of single star polymers, gels of the blend show a slight haziness. Smaller departures from calculated viscosities are also observed when the low-MW star polymer represents only 9% of the polymer mass.

4. Fuzzy Star Polymers. As described in the Experimental Section, two star polymers were prepared that contained 32 arms of 60 000 polybutadiene and 32 arms of 42 000 and 22 000 polybutadiene, respectively. The inner part of these stars is therefore a 64-arm star, but the outer shell consists of only 32 arms. The intrinsic viscosities of these two samples are given in Table 1. The concentration dependence of the relative viscosities of the fuzzy stars is shown in Figure 9. Although measurements were made up to 6 times the overlap volume fraction, no steep increase in the viscosity with concentration and no gel formation are observed. In fact the data for the two fuzzy stars are identical within experimental error with the results obtained on 32-arm stars as shown in Figure 5.

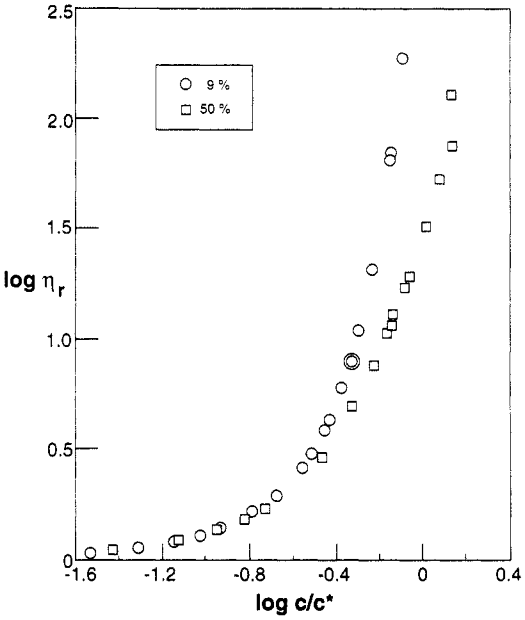

Figure 7. Double-logarithmic plot of the relative viscosity against volume fraction for blends of 12880 and 12807. Symbols: (○) blend with 9 wt % 12807; (□) blend with 50 wt % 12807.

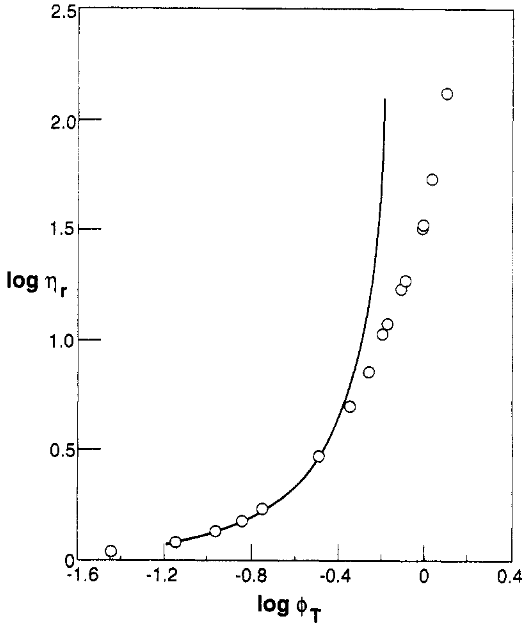

Figure 8. Comparison of the relative viscosity of the 50/50 blend of 12880 and 12807 with the mean-field model of Farris. The line represents eq 5 with $\phi_p = 0.60$. Circles: experimental data.

5. Diblock Copolymer Star. A 64-arm diblock copolymer star with an inner core composed of polybutadiene arms with MW = 20 000 and an outer shell of polystyrene arms with MW = 10 000 was investigated.

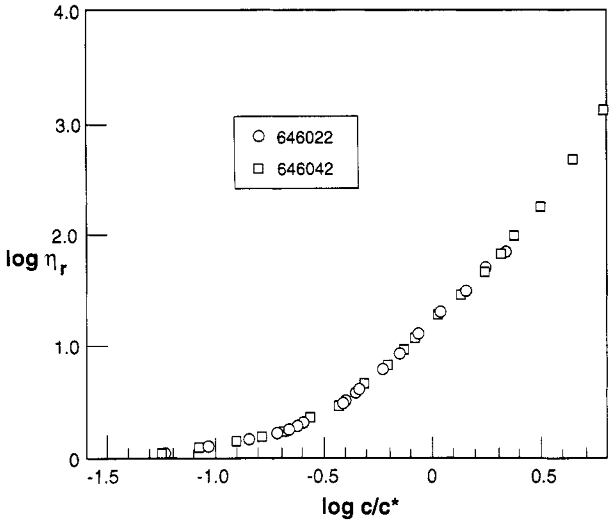

Figure 9. Double-logarithmic plot of the relative viscosity against volume fraction of two fuzzy star polymers.

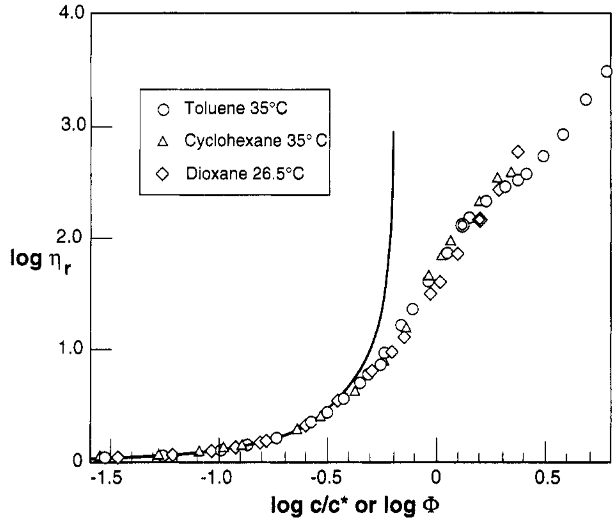

Figure 10. Double-logarithmic plot of the relative viscosity against volume fraction for a 64-arm poly(styrene-*b*-butadiene) star. The solid line represents eq 4 with $\phi_p = 0.65$.

Most extensive relative viscosity data were collected in toluene which is a good solvent for both blocks. The results are shown in Figure 10. The volume fraction has been calculated with the experimental intrinsic viscosity of the block copolymer star. As can be seen in Figure 10, there is no evidence for gel formation in the case of this diblock copolymer. The relative viscosities of the diblock star show a shoulder when the star volume fraction is between 2 and 3 times the overlap volume fraction. The lower relative viscosity is also apparent below the overlap volume fraction when Figure 10 is compared with the results for a regular 64-arm star in Figure 4.

In order to investigate the reasons for the peculiar behavior of the diblock star, experiments were also performed in cyclohexane, a selective solvent for polybutadiene and a Θ-solvent for polystyrene at 35 °C, and in *p*-dioxane, a Θ-solvent for polybutadiene at 26.5 °C and a good solvent for polystyrene. The results are also shown in Figure 10. In the case of cyclohexane the relative viscosity vs concentration curve follows very closely the results obtained in toluene. In the case of *p*-dioxane the relative viscosity increases smoothly with concentration and approximately joins the viscosities of the polymer in the two other solvents in the region of high polymer overlap.

Discussion

The viscosity of solutions of linear and of star polymers with few arms increases gradually with concentration near the polymer overlap concentration. Indeed, while the hydrodynamic interactions between these polymer coils increase with concentration the effects are partly offset by the onset of polymer coil contraction that occurs in semidilute solutions in a good solvent. A stronger dependence of the viscosity of linear and star polymers with concentration is only observed when the polymer concentration reaches a second critical concentration $c^{**} > \rho M_e/M$, where the polymer coils begin to form entanglements.[21,22] While c^* is determined from dilute solution characteristics, c^{**} depends on the characteristic melt entanglement molecular weight (M_e) of the polymer. The results in this study show that the features of the concentration dependence of the relative viscosities of star polymers with $f \leq 32$ are essentially those of linear polymers.

From SANS it is known that some ordering occurs in 32-arm star solutions in good solvents near the overlap concentration and in semidilute solution. However, from the amplitude of the Bragg scattering maximum the ordering is considered liquidlike.[6] Therefore, while 32-arm star polymer coils interact strongly hydrodynamically near and above the overlap concentration and gradually interpenetrate as the concentration increases, the viscosity of the solution is always finite.

A different behavior is observed in the case of the 64- and 128-arm regular stars and in the 270-arm stars. Near the overlap concentration, the Bragg scattering peak maximum of the 64- and 128-arm stars is very high, indicating the formation of a macrocrystalline lattice of the polymer coils.[6] The case of the 270-arm stars has not been investigated. It is exactly under these conditions that strong increases of the relative viscosity with concentration occur and gel formation is observed.

The liquid–gel transition, expressed in terms of volume fraction, decreases from 0.90–1.00 for 64-arm stars to 0.62–0.72 for 128-arm stars and 0.67 for the high-MW 270-arm star. This indicates that a small interpenetration of the coronas of the 64-arm star must occur before they lock into a gellike solid material. In the case of the 270-arm star the liquid–gel transition volume fraction is very nearly that expected for a random close packing of hard spheres. This suggests that little or no interpenetration of the polymer coils is required in order to obtain the solidlike properties.

The importance of a high segment density in the outer periphery of the star polymer coils for ordering and gel formation is brought out by the results on the fuzzy stars. Their behavior is essentially that of 32-arm stars. It can be calculated from the results on regular 64-arm star polymers that the inner cores of the fuzzy stars 646022 and 646042 would begin to overlap at $c/c^* = 2.37$ and 1.45 respectively. However, no abnormal increase of the viscosity with concentration is observed in that concentration range.

The experiments on the blends of two 128-arm star polymers with different sizes are of interest, because the results shed light on the effect of possible contaminants. Furthermore, the results indicate that the relative viscosities of the blends are lower than in the case of hard-sphere particle suspensions as calculated by the model of Farris. At present only a qualitative explanation of the lower viscosity can be offered. It should first be realized that in all cases, also in the 50/50 blend, the volume fraction of 12880 is considerably larger than that of 12807 and that the fraction of 12880 contributes most to the overall viscosity. In the presence of small stars with their associated high osmotic pressure, the large stars are experiencing the surroundings of a thermodynamically weaker solvent than in the case of pure solvent. Relative to the pure solutions case, the large star coils are therefore smaller and a reduced viscosity of the solution is observed. By keeping the weight ratio of the two stars constant, the solvent quality becomes progressively poorer as the total polymer concentration increases. In order to quantify the effect of added polymer on the solvent quality, it would be preferable to perform experiments in which the (linear or other) polybutadiene concentration is kept constant and the star polymer concentration is varied.

Finally, some qualitative comments are required with respect to the results obtained with the diblock star polymer. It should be realized that the polybutadiene block constitutes the larger volume fraction of the star because it has the largest mass and a larger characteristic ratio and is more stretched in the core of the star than the polystyrene block. This can also be deduced from $[\eta]$ = 69.6, 60.6, and 38.9 in toluene, cyclohexane, and dioxane, respectively. The shoulder in the viscosity concentration curve of the diblock star in toluene is ascribed to the shrinking of the polybutadiene block when the total polymer concentration increases. This would be similar to the phase inversion observed during the synthesis of high-impact polystyrene. This hypothesis is supported by a similar pattern in cyclohexane. However, the viscosity–concentration curve in dioxane is smooth as expected for a Θ-solvent for polybutadiene. The small polystyrene chains are not expected to play a major role.

References and Notes

(1) Roovers, J.; Zhou, L.-L.; Toporowski, P. M.; van der Zwan, M.; Iatrou, H.; Hadjichristidis, N. *Macromolecules* **1993**, *26*, 4324.
(2) Batchelor, G. K. *J. Fluid Mech.* **1977**, *83*, 97.
(3) Willner, L.; Jucknischke, O.; Richter, D.; Roovers, J.; Zhou, L.-L.; Toporowski, P. M.; Fetters, L. J.; Huang, J. S.; Lin, M. Y.; Hadjichristidis, N. *Macromolecules* **1994**, *27*, 3821.
(4) Daoud, M.; Cotton, J.-P. *J. Phys.* (*Les Ulis, Fr.*) **1982**, *43*, 531.
(5) Witten, T. A.; Pincus, P. A.; Cates, M. E. *Europhys. Lett.* **1986**, *2*, 137.
(6) Richter, D.; et al. *Polym. Mater. Sci. Eng.* **1992**, *67*, 425.
(7) Krieger, I. M. *Adv. Colloid Interface Sci.* **1972**, *3*, 111.
(8) Ball, R. C.; Richmond, P. *Phys. Chem. Liq.* **1980**, *9*, 99.
(9) Tsenoglou, C. *J. Rheol.* **1990**, *34*, 15.
(10) Zhou, L.-L.; Roovers, J. *Macromolecules* **1993**, *26*, 963.
(11) Zhou, L.-L.; Hadjichristidis, N.; Toporowski, P. M.; Roovers, J. *Rubber Chem. Technol.* **1992**, *65*, 303.
(12) Roovers, J.; Toporowski, P.; Martin, J. *Macromolecules* **1989**, *22*, 1897.
(13) Toporowski, P. M.; Roovers, J., to be published.
(14) Van Wazer, J. R.; Lyons, J. W.; Kim, K. Y.; Colwell, R. E. *Viscosity and Flow Measurements*; Interscience Publishers: New York, 1963.
(15) Mewis, J.; D'Haene, P. *Makromol. Chem., Macromol. Symp.* **1993**, *68*, 213.
(16) Roovers, J. *Macromolecules* **1991**, *24*, 5895.
(17) Utracki, L.; Simha, R. *J. Polym. Sci., Part A* **1963**, *1*, 1089.
(18) Simha, R.; Utracki, L. *J. Polym. Sci., Polym. Phys. Ed.* **1967**, *5*, 853.
(19) Utracki, L. A.; Roovers, J. *Macromolecules* **1973**, *6*, 366.
(20) Farris, R. J. *Trans. Soc. Rheol.* **1968**, *12*, 281.
(21) Berry, G. C.; Fox, T. G. *Adv. Polym. Sci.* **1968**, *5*, 261.
(22) Graessley, W. W. *Polymer* **1980**, *21*, 258.